Nuclear spectroscopy with lithium beams. I. High-spin states in ^{55}Fe, ^{55}Mn, and ^{53}Cr†

A. R. Poletti*
University of Auckland, Auckland, New Zealand

B. A. Brown‡ and D. B. Fossan
State University of New York, Stony Brook, New York 11790

E. K. Warburton
Brookhaven National Laboratory, Upton, New York 11973

(Received 13 August 1974)

The ^{7}Li bombardment of ^{51}V has been used in conjunction with recoil distance lifetime (RDM), γ-γ coincidence, angular distribution, and Doppler shift attenuation lifetime (DSAM) measurements to gain information on the properties of high-spin states in the nuclei ^{55}Fe, ^{55}Mn, and ^{53}Cr. Mean lifetimes (τ) determined by RDM were as follows—in ^{55}Fe: 1409-keV level ($\tau = 57.8 \pm 3.5$ psec), 2813 (14.5 ± 3.1 psec), 5099 (32.3 ± 1.1 psec); in ^{55}Mn: 126-keV level ($\tau = 382 \pm 16$ psec); in ^{53}Cr: 2173-keV level ($\tau = 47 \pm 15$ psec); 3084 ($\tau = 43 \pm 15$ psec). Tentative spin assignments were made as follows—in ^{55}Fe: 5099-keV level $J = (\frac{19}{2})$, 6528, $J = (\frac{21}{2})$, in ^{55}Mn: 3056-keV level $J = (\frac{15}{2})$. Lifetimes (or limits) were also established from DSAM measurements for a number of other levels in the above nuclei. The results are compared to shell model calculations.

[NUCLEAR REACTIONS ^{51}V(^{7}Li, $3n$), ^{51}V(^{7}Li, $p2n$), ^{51}V(^{7}Li, αn) $E = 25$ MeV; measured $\gamma\gamma$ coin.; deduced levels in ^{55}Fe, ^{55}Mn, ^{53}Cr; measured $\sigma(E_\gamma, \theta)$; deduced J^π for high spin states; measured recoil distance; deduced $T_{1/2}$, $B(E2)$, effective charges. Natural target, Ge(Li) detectors.]

INTRODUCTION

In nuclei near closed shells with only a few valence particles, the low-lying high-spin states are expected to be rather pure in the shell model sense. An experimental determination of the level energies and spins for specific configurations in a given nucleus can therefore give valuable information on the interaction matrix elements of the residual forces. In addition, measurements of the lifetimes of these levels allow the determination of the electromagnetic transition matrix elements which give information on their effective operators. Both of these experimental studies in turn are sensitive to the configurations involved in the nuclear structure. An interesting region from these points of view is where the proton $1f_{7/2}$ shell is filling with the $1f_{7/2}$ neutron shell complete plus at most a few valence neutrons in the $(1f_{5/2}, 2p)$ shell. Until very recently, the predictions of shell model calculations concerning the properties of the expected high spin states could not in general be tested. Not only did this inhibit the publication of such predictions, but also the predictions of the model in an important area perforce remained untried. The reason for this state of affairs lay in the rather limited range of projectiles available for exciting the levels in question. With the wider availability of heavy ion beams for fusion-evaporation reactions together with large volume Ge(Li) γ-ray spectrometers, levels of high spin are now much more easily excited and observed.[1]

High-spin states in a number of nuclei in this $(1f, 2p)$ region of interest are populated by the bombardment of ^{51}V with ^{6,7}Li at around 25 MeV followed by multiparticle emission. That this leads to the population of high-spin states can easily be seen. Classically a 14-MeV proton incident with an impact parameter equal to the nuclear radius of ^{51}V carries approximately 4 units of angular momentum into the compound nucleus whereas a 25-MeV ^{7}Li ion similarly incident carries 12 units. This in itself is not sufficient to ensure the population of high spin levels in specific residual nuclei; for instance a heavy product nucleus could just as easily carry away from the compound nucleus all the angular momentum contributed by the incident particle. That this does not happen is due to two factors: (i) The emission probability is proportional to the density of states of the residual nucleus at the energy corresponding to the emission energy of the particle.[2] (ii) In addition, this probability depends very sensitively on the Coulomb barrier for charged particle emission. The density of states is high only for the emission of low energy particles. The most likely mode of deexci-

tation in the heavier nuclei is therefore the emission of a few neutrons. Each such low energy neutron, being a light particle, will be unable to carry away any substantial amount of angular momentum from the compound nucleus. However, for nuclei in the $A \approx 50$ region the Coulomb barrier is not so high as to inhibit completely the emission of charged particles; hence the emission of both protons and α particles is also probable. The effect of the Coulomb barrier is, however, to make the multiple emission of charged particles extremely unlikely.

The energetics of the reactions of interest to us are sketched in Fig. 1. An incident ^{7}Li beam bombarding ^{51}V with an energy of 25 MeV corresponds to an excitation energy of 46.8 MeV in the compound nucleus ^{58}Fe. At this energy the most strongly excited residual nuclei corresponded to those obtained by two or three particle emission. These were (in descending intensity of excitation): ^{55}Fe $(-3n)$; ^{52}Cr $(-\alpha 2n)$; ^{55}Mn $(-p2n)$; ^{53}Cr $(-\alpha n)$ and ^{56}Fe $(-2n)$. Their relative excitation intensities using an infinitely thick target were 60 : 50 : 28 : 28 : 24. More weakly excited was ^{54}Mn $(-p3n)$ whose relative excitation intensity was 6. It is noteworthy that the nuclei corresponding to single particle emission [^{57}Fe $(-n)$; ^{57}Mn $(-p)$ and ^{54}Cr $(-\alpha)$] were not observed at all. No nucleus whose formation involved the multiple emission of charged particles was directly observed. Probably, however, ^{53}V was formed as evidenced by the observation of effects on some of the γ rays in ^{53}Cr which could best be explained by their partial production through the β decay of ^{53}V. The observation of ^{54}Mn and not ^{54}Fe can be ascribed to the comparatively low excitation energies of high-spin states in the former nucleus. In a subsidiary experiment, ^{51}V was bombarded with ^{6}Li at the same energy of 25 MeV. The nuclei most strongly excited in this case were ^{52}Cr $(-\alpha n)$, ^{54}Mn $(-p2n)$, and ^{54}Fe $(-3n)$ with ^{55}Fe and ^{55}Mn more weakly excited. In general, at the bombarding energies used in this experiment, the most likely reactions are those involving the emission of three particles, no more than one being charged. Two-particle emission is somewhat weaker and four-particle emission is likely only in certain favored cases.

Once the residual nuclei reach an excitation energy which is low enough so that particle emission is no longer probable, their γ-ray decay to the ground state can be understood in terms of the concept of yrast levels first introduced by Grover.[3] An yrast level is the lowest-lying level for a given spin. Once an yrast level is reached the nucleus will usually deexcite by the emission of dipole and quadrupole radiation through successive yrast levels. This cascade down the yrast line has two important experimental consequences. The first is that the average γ-ray energy is rather low. (For ^{55}Fe in this experiment, the average observed γ ray energy was 900 keV.) A result of this is that a number of the levels will have mean lifetimes greater than 10 psec, a range which is accessible to the recoil distance method (RDM) for lifetime measurements. (For $A = 55$, a 900-keV transition has a mean lifetime of 12 psec if it is an $E2$ typically enhanced 10 times over the Weisskopf single particle estimate,[4] whereas an $M1$ transition inhibited by a not uncommon factor of 100 from the single particle estimate[4] has a mean lifetime of 4.3 psec.) Some transitions will have lifetimes too short to measure by the RDM method. In these cases the Doppler shift attenuation method (DSAM) often enables an experimenter to determine the lifetime. The second consequence is that the high γ-ray multiplicity means that a γ-γ coincidence measurement is essential if the energy levels are to be correctly placed in the residual nucleus. It is often also vital in assigning a particular γ ray to its correct nucleus.

Heavy ion induced compound reactions produce considerable alignment in the residual nucleus, because the large amount of angular momentum carried into the compound nucleus is oriented at right angles to the beam. Since the γ-ray transitions deexciting the yrast levels are in general stretched ($J \rightarrow J - L$, where L is the multipolarity of the γ ray), this implies that quite significant

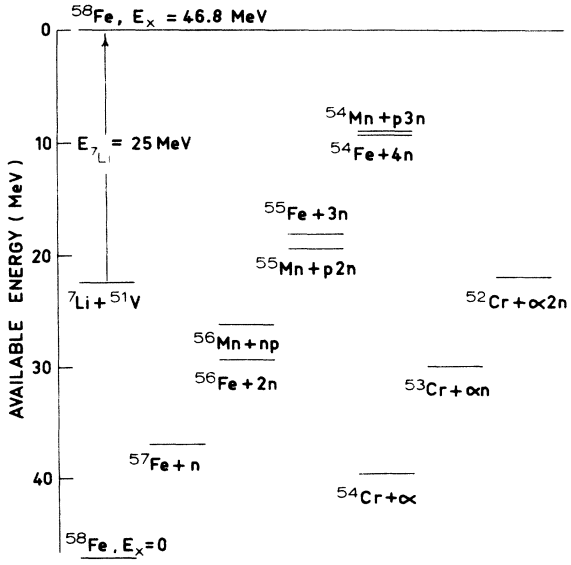

FIG. 1. The energy relationships involved when a ^{51}V target is bombarded with ^{7}Li at an energy of 25 MeV. At this energy the most strongly excited nuclei were ^{55}Fe, ^{52}Cr, ^{55}Mn, and ^{53}Cr. ^{56}Fe and ^{54}Mn were also excited, the latter quite weakly.

information on the spins of the levels concerned can be obtained from the angular distributions of the observed γ rays. In this and the succeeding paper all tentative spin assignments which we make will depend on two assumptions, viz: that it is the yrast levels which are populated mainly in low magnetic substates, and that the subsequent γ-ray transitions are pure $J \rightarrow J - L$ transitions.

In order to obtain nuclear structure information on high-spin states in this region, we therefore undertook measurements of the following type on the γ rays resulting from ^{7}Li bombardment of ^{51}V at about 25 MeV: (1) recoil distance lifetime measurements, (2) γ-γ coincidence measurements, (3) angular distribution measurements, and (4) Doppler shift attenuation lifetime measurements. A large amount of information was thus acquired on the properties of excited states in six nuclei. In this first paper we discuss the properties of the odd nuclei ^{55}Fe, ^{55}Mn, and ^{53}Cr. A second paper[5] will treat the nuclei ^{52}Cr, ^{54}Mn, and ^{56}Fe. Information gained on the nuclei ^{54}Mn and ^{54}Fe by bombarding ^{51}V with ^{6}Li will also be discussed in the second paper.

EXPERIMENTAL

Ions of ^{7}Li provided by the injector tandem accelerator at Brookhaven National Laboratory, with energies between 24 and 25 MeV, were used to bombard targets of ^{51}V. The γ rays resulting from this bombardment were observed with the aid of Ge(Li) γ-ray spectrometers. We used standard modular electronics and stored our data using the on-line Σ-7 computer of the tandem facility. We will now describe each type of experiment and the data analysis in more detail.

A. RDM experiment

The apparatus described by Jones, Schwarzschild, Warburton, and Fossan[6] was used together with a ^{51}V target of 300-μg/cm^2 thickness evaporated on the downstream side of a gold foil of 3-mg/cm^2 thickness. This target was stretched flat. Target-stopper distances of up to 5 mm were used; however, most of the data were recorded at distances of less than 250 μm. For each target-stopper distance the γ-ray spectrum was observed at 0° with a Ge(Li) spectrometer. Typically, each run lasted an hour with a beam current of 4 nA of $^{7}Li^{3+}$ ions. The beam energy of 25 MeV gave an effective energy, after allowing for energy loss in the gold foil, of 24 MeV at the ^{51}V target. The lifetime determined from an RDM experiment depends directly on the velocity of the recoiling nuclei. For a heavy ion reaction in which several low energy light particles are emitted following compound nucleus formation, this recoil velocity would be expected to be very close to the center of mass (c.m.) velocity. This was indeed so for the cases in ^{55}Mn and ^{56,55}Fe where we could make the check as measured by the energy shift between the stopped and shifted γ-ray peaks. After correcting for the energy loss of the ^{7}Li ions in the gold foil and target and the average energy loss of the recoiling ions in the ^{51}V target layer, the calculated c.m. velocity was $100\bar{v}/c = 0.91 \pm 0.02$. For six transitions in the mass 55 and 56 nuclei, the observed weighted average was $100\bar{v}/c = 0.849 \pm 0.008$. We used this figure in extracting all the lifetimes in the mass 54–56 nuclei. There was, however, definite evidence that the average recoil velocities for ^{52,53}Cr were substantially less than the calculated c.m. velocity; for ^{53}Cr, the velocity as measured by γ-ray energy shifts was $100\bar{v}/c = 0.36 \pm 0.03$, while for ^{52}Cr the corresponding figure was $100\bar{v}/c = 0.708 \pm 0.007$. The very low recoil velocities observed for the chromium isotopes will be discussed below.

B. γ-γ coincidence measurements

A piece of ^{51}V metal 0.38-mm thick was used as the target. We used two Ge(Li) spectrometers placed at ±110° with respect to the beam direction which had efficiencies for 1.33-MeV γ rays of 6% and 12%. A fast-slow coincidence system using standard modular electronics was used. The resulting two parameter data were stored on magnetic tape in an event-mode fashion for later playback using the Σ-7 computer. The run lasted 20 h with a beam current of about 1 nA of 25-MeV $^{7}Li^{3+}$ ions.

C. Angular distribution measurements

γ-ray spectra were accumulated using the 12% detector at a distance of 13.5 cm from the target (same as in Sec. B) and at angles of 0, 30, 45, 60, and 90° with respect to the beam direction. The smaller detector was placed at 90 and used as a monitor. A beam current of about 4 nA of $^{7}Li^{3+}$ ions at 25 MeV was used. Spectra were recorded at each angle for approximately 35 min. Information on the Doppler shifts of γ rays was, of course, also contained in this data. It was used in later DSAM analysis.

DATA ANALYSIS

In all four experiments, the primary requirement was to obtain the areas and/or centroids of the peaks of interest. As an illustration of the spectra upon which we had to work, we show in Fig. 2 a γ-ray spectrum obtained in the angular

distribution experiment at an angle of 90°. The richness of the spectrum is obvious. We have been able to place more than 60 γ-ray transitions in six different nuclei. The origin of the stronger peaks is indicated on the diagram. For isolated peaks it was merely necessary to find the centroid and area after a least squares fitting to the background. In the case of overlapping and partially resolved peaks, it was necessary to use a least squares program which after background subtraction could fit up to three Gaussian peaks. Constraints could be placed on the positions of the centroids of these peaks.

For the RDM measurements, where possible, we then formed the ratio $R = I_0/(I_0 + I_s)$ where I_0 and I_s are the intensities of the stopped and shifted peaks, respectively. Comparable lifetime information can also be obtained from I_0 or I_s alone, provided a suitable normalization is used. For this purpose we used the sum (N) of the areas of the γ-ray peaks at 126, 156, and 212 keV, fitting the quantities $R_0 = I_0/N$ or $R_s = I_s/N$.

The quantity R is easily seen to depend in the simplest case on the mean life τ of a level in the following manner[6,7]:

$$R = \exp[-(D - D_0)/\bar{v}\tau] , \qquad (1)$$

where $\bar{v}$ is the average recoil velocity, D_0 is the reading on the dial gauge corresponding to zero plunger-to-target distance and D is the corresponding reading when the plunger is displaced a distance $(D - D_0)$ from the target. There is often a distance-independent background resulting in an R that is not unity at $D = D_0$. We, therefore, used an iterative nonlinear least squares code to fit $R = Ae^{-D/\bar{v}\tau} + B$ to the data, leaving the quantities A, τ, and B to be determined by the fitting procedure. In this case $e^{D_0/\bar{v}\tau}$ is absorbed into the variable A. The same form could also be used to fit R_0 or R_s. In the latter case, of course, we could expect A to be negative. A number of small corrections need to be made to this simple analysis. We corrected R for the change in efficiency of the Ge(Li) detector as a function of energy, solid angle effects, and the spread in velocity of the recoiling nuclei. Errors of ±1.5 μm were assigned to the uncertainty in the relative distance settings. For a transition which is affected by the lifetimes of two levels, we fitted R (or R_0) to an expression of the form

$$R = A\exp(-D/\bar{v}\tau_1) + C\exp(-D/\bar{v}\tau_2) + B , \qquad (2)$$

where we could fix τ_1 from a direct measurement on the γ ray deexciting the first level. Several such cases were encountered in this work.

For the γ-γ coincidence experiment all coincident events were first projected onto one energy axis to give a "summed" spectrum. Suitable digital peak and background windows were then set on the event addresses corresponding to this axis and the corresponding spectra accumulated in a playback of the data. Forty-seven such spectra were thereby accumulated for the strongest peaks seen in the original summed spectrum.

The areas of the peaks obtained at each angle in the angular distribution experiment were normalized to the counts recorded in the 274-keV peak observed in the monitor detector, corrected for dead time and counter efficiency. They were then fitted to a function of the form

$$W(\theta) = I_\gamma[1 + a_2P_2(\cos\theta) + a_4P_4(\cos\theta)] \qquad (3)$$

to obtain the intensity I_γ (corrected for detector efficiency) and the values of the Legendre poly-

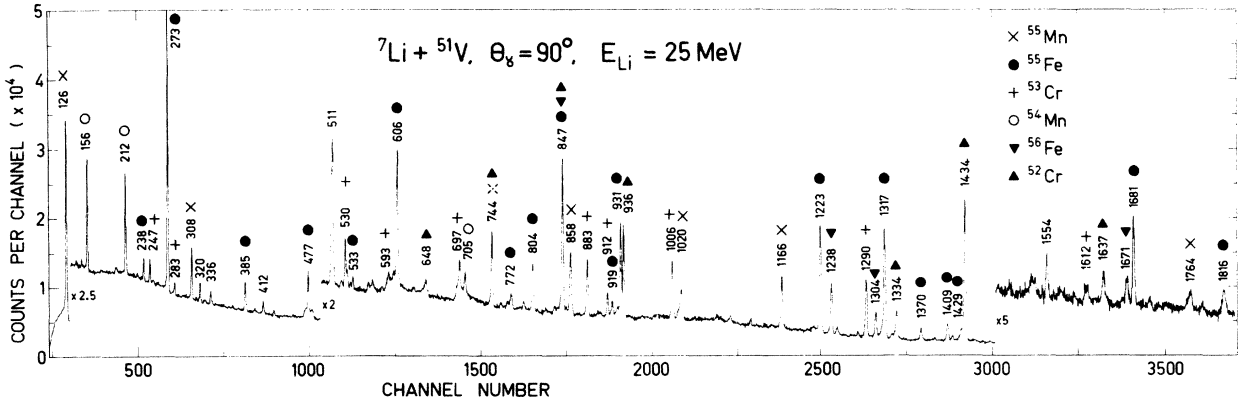

FIG. 2. The γ-ray spectrum observed in a Ge(Li) spectrometer at 90° to the beam when a thick target of ^{51}V is bombarded with 25-MeV ^{7}Li. As indicated on the figure, γ rays in six nuclei were seen. These were ^{55}Mn, ^{55}Fe, ^{53}Cr, ^{54}Mn, ^{56}Fe, and ^{52}Cr. γ-ray energies are in keV. We were able to assign all transitions except for some of the weaker ones.

nomial coefficients a_2 and a_4. Some of the transitions were too weak to obtain I_γ from the angular distribution data. For these cases intensities were estimated from the γ-γ coincidence data and are indicated by the symbol ~ in the tables. The relative intensities I_γ were used in constructing the various decay schemes. Errors on the branching ratios (in percent) from individual levels in the different nuclei (as derived from the relative intensities given in Figs. 3, 6, and 8) are $\approx \pm 2\%$. The values of a_2 and a_4 have been used to assign tentative spins to some of the higher lying levels and to check assignments of lower levels. We were guided in this by the fact[1,8] that for the $J \to J - L$ decays from highly aligned levels which we have assumed (see Introduction), dipole transitions have negative a_2 coefficients while for the stretched quadrupole transitions a_2 is positive and a_4 is smaller and negative.

The centroids of peaks of interest in the DSAM experiment were also obtained wherever there was a possibility of a Doppler shift. These, generally after some correction for cascade feeding from higher excited states, were used to calculate $F(\tau)$, the fractional Doppler shift. A program[9] which took account of electronic stopping and atomic stopping and scattering was used to obtain τ from $F(\tau)$.

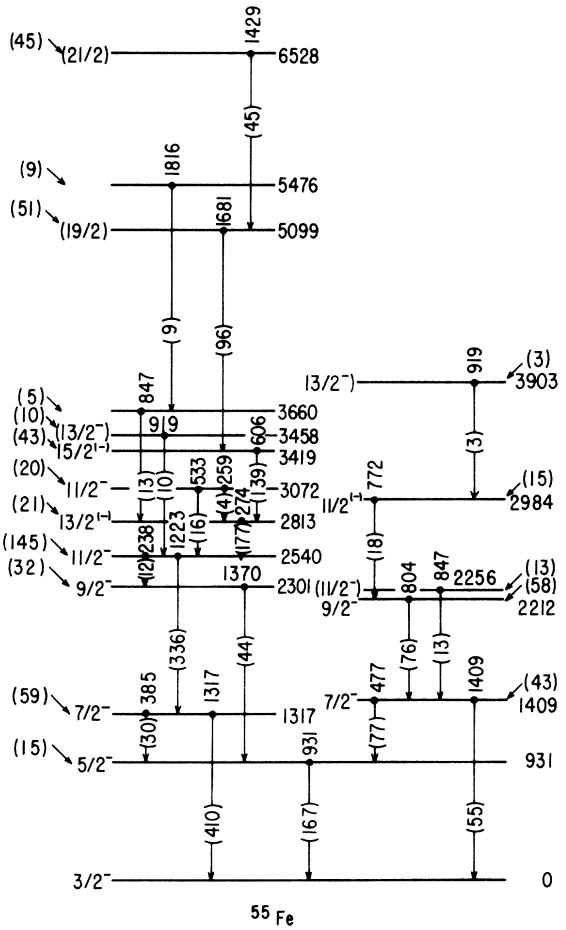

FIG. 3. The energy level diagram of ^{55}Fe. The energies of all observed γ-ray transitions are shown at the top of the arrow indicating the transition, while relative intensities of observed γ rays are indicated by the bracketed numbers in the middle of the arrows. The bracketed numbers at both sides of the figure indicate the relative intensities of excitation of the levels concerned. The diagram includes only those levels excited in the present work. Levels shown to the right are believed to be built on the deformed Nilsson orbital $[303]\frac{7}{2}^-$ while those on the left are shell-model states. Of major interest are the three highest excited states first seen in the present work. The analysis of γ-ray angular distributions indicates that their spins are rather high. The two spin values in parenthesis for the levels above 4-MeV excitation are especially tentative and, in fact, only suggestions.

RESULTS

A. ^{55}Fe

The γ-γ coincidence measurement confirmed the energy level scheme proposed by Sawa[10] for all the levels up to an excitation energy of 3900 keV. The γ-ray energies determined in the present work are presented in Table I and are in general in good agreement with those presented by Sawa.[10] In addition, the transition assignments are given in columns 2 and 3. We give the derived energy levels in Table II. We were able to establish the presence of three new levels at considerably higher excitation energies than those observed by Sawa[10]: 5099, 5476, and 6528 keV. Combining lifetime and angular distribution information we assign tentative spins of $(\frac{19}{2})$ and $(\frac{21}{2})$ to the 5099- and 6528-keV levels, respectively. The energy level and decay scheme for ^{55}Fe as obtained in the present work is shown in Fig. 3. The energy levels in Fig. 3 are split into two groups as presented by Sawa.[10] Those on the left are believed to be normal shell-model states while the levels on the right, that are connected by cascade γ rays, have been interpreted[10] as possible rotational levels built on a deformed neutron-hole state at 1409 keV. The level energies are given in keV, while γ-ray energies (also in keV) are shown at the tops of the arrows signifying the transition. The numbers in brackets in the middle of each arrow give the relative intensity of the γ ray concerned, while the bracketed numbers to the left and right of the figure give the relative intensities of excitation of the individual levels. Columns 4 and 5 of Table I list the coefficients of the Legendre polynomials, while the last column gives the relative intensities of the observed γ rays (corrected for detector efficiency).

TABLE I. γ-ray transitions in ^{55}Fe seen in the ^{51}V(^{7}Li, $3n$)^{55}Fe reaction.

E_γ (keV)	E_i	E_f	a_2	a_4	I_γ
238.3 ± 0.2	2.54	2.30	−0.29 ± 0.04	0.06 ± 0.05	119 ± 3
259.2 ± 0.5	3.07	2.81	...	...	...
273.6 ± 0.2	2.81	2.54	−0.17 ± 0.01	−0.03 ± 0.01	1770 ± 13
385.3 ± 0.2	1.32	0.93	−0.21 ± 0.03	−0.06 ± 0.03	300 ± 6
477.2 ± 0.2	1.41	0.93	−0.02 ± 0.03	−0.04 ± 0.03	774 ± 13
532.9 ± 0.3	3.07	2.54	...	...	...
605.6 ± 0.2	3.42	2.81	−0.19 ± 0.02	−0.01 ± 0.02	1391 ± 14
772.2 ± 0.3	2.98	2.21	...	...	...
803.6 ± 0.3	2.21	1.41	−0.11 ± 0.03	−0.07 ± 0.03	763 ± 14
847 ± 1.0	2.26	1.41	...	...	...
	3.66	2.81	...	...	...
918.7 ± 0.6	3.90	2.98	...	...	...
	3.46	2.81	...	...	...
931.4 ± 0.2	0.93	0	0.10 ± 0.02	−0.05 ± 0.02	1671 ± 19
1222.8 ± 0.3	2.54	1.32	0.26 ± 0.01	−0.09 ± 0.02	3358 ± 26
1316.8 ± 0.3	1.32	0	0.19 ± 0.01	−0.09 ± 0.02	4098 ± 33
1369.8 ± 0.4	2.30	0.93	0.17 ± 0.05	−0.18 ± 0.05	445 ± 12
1408.5 ± 0.3	1.41	0	0.11 ± 0.03	−0.03 ± 0.03	548 ± 9
1429.0 ± 1.0	6.53	5.10	...	...	...
1680.6 ± 0.4	5.10	3.42	0.42 ± 0.02	−0.15 ± 0.02	959 ± 12
1816.0 ± 2.0	5.48	3.66	−0.41 ± 0.12	0.17 ± 0.12	287 ± 11

It will be seen that although the spins of the target and projectile were quite high ($\frac{7}{2}$ and $\frac{3}{2}$, respectively), there was still a considerable alignment achieved, especially for the higher spin levels. The angular distribution coefficients listed in the table are consistent with the spins proposed by Sawa.[10] Of the three new transitions observed by us in this nucleus we were able to determine angular distributions for two of them: the large positive a_2 and significant negative a_4 obtained for the 1681-keV transition from the 5099-keV level is consistent with it being a quadrupole transition and with the spin of the 5099-keV level being $\frac{19}{2}$, while the large negative a_2 for the 1816-keV transition is consistent with a $(J \rightarrow J-1)$ dipole transition.

We were able to determine the lifetimes of three levels in this nucleus using the RDM method, while upper and lower limits could be set on the lifetime of a fourth. The results for two of these are shown in Fig. 4. The 1681-keV γ ray showed a very clear lifetime effect. The three lower partial γ-ray spectra in the figure are representative of those which we analyzed to obtain the lower lifetime curve. This curve was well fitted with a single exponential term yielding a mean lifetime for the 5099-keV level in ^{55}Fe of 32.3 ± 1.1 psec. (In order to display this clearly, a small distance-independent background R_∞ has been subtracted from the values of R calculated directly from the data.) The 606-keV transition deexciting the 3419-keV level showed two lifetime components. A prompt contribution was documented by a Doppler shape in the angular distribution while a feeding lifetime, obtained from the RDM results, was consistent with the lifetime of the 5099-keV level. The mean lifetime of the 3419-keV level was determined as 0.1 ± 0.03 psec in the DSAM measurements. (It should be emphasized that all mean lifetimes of ≤1 psec are really upper limits on the lifetime because of the unknown feeding time.[1])

The 274-keV transition following the 606-keV γ ray showed evidence of two lifetimes. Representative partial spectra displaying the stopped and shifted photopeaks of this transition are shown in the upper part of Fig. 4. The peak indicated by the arrow at channel 737 is due to the gold backing as is the intense 379-keV γ ray. The data representing $R - R_\infty$ derived from the analysis of these and the other spectra is displayed in the top left-hand corner of the figure. For distances greater than 80 μm this curve shows the same lifetime as the lower curve. We ascribe the upward warping of the curve at smaller distances to the fact that the 2813-keV level has a mean lifetime of 14.5 ± 3.1 psec, the value obtained by fitting an expression of the form of Eq. (2) to the data. The value of τ_1 in this fit was fixed as $\tau_1 = 32.3 \pm 1.1$ psec.

The 1223-keV γ ray deexciting the 2540-keV level was fed by the 274-keV transition. This transition showed a very distinct lifetime effect as can be seen from the partial spectra shown in the bottom of Fig. 5. The derived quantity $R - R_\infty$ is plotted to the left. This could be fitted by one exponential term and yielded a value of $\tau = 21.8 \pm 1.0$ psec.

TABLE II. Energies and lifetimes of excited states in ^{55}Fe populated by the ^{51}V(^{7}Li, $3n$)^{55}Fe reaction.

E_x (keV)	$F(\tau)$ [a]	τ (psec) Present work	τ (psec) Other	τ (psec) Adopted
931.4 ± 0.2		...		
1316.8 ± 0.3	<0.67	>0.16	$0.91^{+0.91}_{-0.31}$ [b] $0.95^{+3.05}_{-0.41}$ [c]	$0.92^{+0.87}_{-0.25}$
1408.5 ± 0.3		57.8 ± 3.5	49 ± 10 [c]	56.8 ± 3.30
2212.1 ± 0.4	0.19 ± 0.04	1.10 ± 0.30	$0.35^{+0.35}_{-0.16}$ [c]	0.75 ± 0.40
2256 ± 1.0		...		
2301.2 ± 0.5			$0.90^{+0.70}_{-0.23}$ [b] >0.74 [c]	$0.90^{+0.70}_{-0.23}$
2539.5 ± 0.4	<0.01	17 ± 6 [d]	>0.66 [b]	17 ± 6
2813.1 ± 0.4		14.5 ± 3.1		14.5 ± 3.1
2984.3 ± 0.5		...		...
3072.3 ± 0.5		>1 [e]		>1
3418.7 ± 0.4	0.78 ± 0.08	0.10 ± 0.03		0.10 ± 0.03
3458.2 ± 0.7	<0.22	>0.9		>0.9
3660 ± 1.1		...		...
3903 ± 0.8	...			...
5099.3 ± 0.6		32.3 ± 1.1		32.3 ± 1.1
5476 ± 2.0	<0.10	>1		>1
6528.3 ± 1.2		<1 [f]		<1

[a] Corrected for feeding from higher lying states.
[b] B. C. Robertson *et al.*, Nucl. Phys. A160, 137 (1971).
[c] Reference 11.
[d] See text.
[e] No Doppler shift observed for the 533 keV γ ray in the angular distribution measurements.
[f] Doppler shifts observed in angular distribution measurements, but unable to measure the shift.

Obviously the lifetimes of the 5099- and 2813-keV levels must be reflected in the RDM data of this 1223-keV transition. However, careful comparison of the three RDM curves shows that the 2540-keV level must have a lifetime greater than that of the 2813-keV level (i.e., $\tau > 11.4$ psec). Obviously, too, $\tau < 22.8$ psec. We conclude that $\tau = 17 \pm 6$ psec. An attempt to extract a more accurate value for this lifetime by making a three component fit to the data was not successful. The last level in ^{55}Fe whose lifetime we could measure using the RDM method was that at 1409 keV. Data for the stronger of the two transitions deexciting this level are shown in the top part of Fig. 5. The values of τ which we obtained from an analysis of the decay curves of both transitions were in good agreement with the average value of τ which we obtained, $\tau = 57.8 \pm 3.5$ psec. The measurement by Robertson, Neilson, and McDonald[11] of this quantity ($\tau = 49 \pm 10$ psec) agrees well with our value. We therefore adopt $\tau = 56.8 \pm 3.3$ psec as the lifetime of this level. Table II contains a lifetime summary.

Information on the lifetimes of several of the levels was obtained from DSAM analysis of the spectra accumulated in the angular distribution experiment. The fractional Doppler shifts, corrected where necessary for feeding from longer lived, higher excited states are given in the second column of Table II. The lifetimes derived from these fractional shifts are shown in the third column. Measurements by other workers are shown in column 4. Except for the RDM measurement of the lifetime of the 1409-keV level, only one other lifetime can be compared directly to the

results obtained by other workers; for the 2212-keV level we are in fair agreement with the measurement of Ref. 11.

B. ^{55}Mn

The γ-γ coincidence measurement confirmed the energy level scheme proposed by Sawa[10] for all the levels up to an excitation energy of 2311 keV. [Sawa had investigated both this nucleus and ^{55}Fe using the ^{52}Cr(α, p) and (α, n) reactions, respectively.] In addition we established the presence of two higher lying states at 2829 and 3056 keV. Figure 6 summarizes the level scheme and decay properties as observed by us. The γ-ray energies determined in the present work are collected in Table III together with the angular distribution coefficients and intensities. The angular distributions which we could observe were rather more isotropic than were those in ^{55}Fe. Their general trend, however, was consistent with the spin assignments of Sawa.[10] The pronounced anisotropy of the angular distribution of the 1764-keV transition from the 3056-keV level suggests that the spin of this state is $(\frac{15}{2})$. This is consistent also with its branching to the $\frac{13}{2}^{(-)}$ state at 2311 keV and the mean lifetime of the level as measured by DSAM of 0.27 ± 0.06 psec. We were unable to obtain the angular distribution of the 1536-keV γ ray deexciting the 2829-keV level. Besides the 3056-keV level, we were able to obtain evidence on the lifetimes of several of the states from the DSAM measurements. These values are listed in Table IV which also gives our best estimates of the energies of the levels excited in this nucleus. We were able to measure the lifetime of the 126-keV level using the RDM method as $\tau = 382 \pm 16$ psec. The lifetime curve and two sample spectra are given in Fig. 7. As can be seen, because of the very low energy of the transition we could not resolve the stopped and shifted peaks in the spectrum. We, therefore, used the Gaussian fitting program with the relative positions of the two peaks fixed (c.f. the discussion

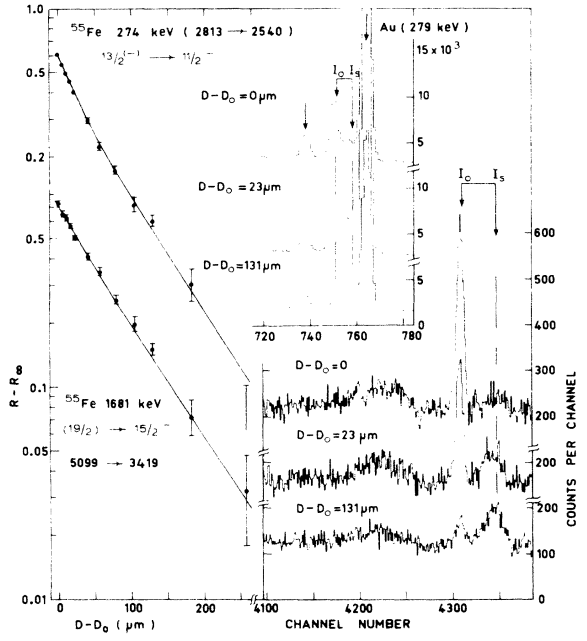

FIG. 4. The results of RDM measurements on two γ-ray transitions in ^{55}Fe. The lower exponential curve and the three associated γ-ray spectra show the data obtained for the 1681-keV transition in ^{55}Fe deexciting the level at 5099 keV. The mean lifetime of the 5099-keV state obtained from an analysis of this data was 32.3 ± 1.1 psec. The upper curve and the associated spectra show the data obtained for the 274-keV transition deexciting the 2813-keV level. The curve through the data points reflects two lifetimes: the longer one being due to the level at 5099 keV, while the shorter lifetime of $\tau = 14.5 \pm 3.1$ psec which causes the slight warping at small plunger distances is ascribed to the 2813-keV level.

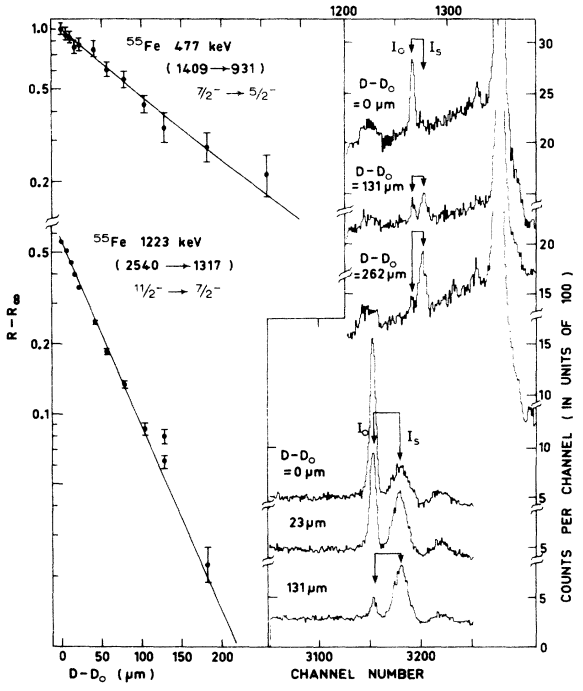

FIG. 5. RDM results obtained for two levels in ^{55}Fe. The upper curve with its associated spectra shows the data obtained for the 477-keV transition from the 1409-keV level. The mean lifetime of the 1409-keV state obtained from an analysis of this data is 57.8 ± 3.5 psec. The lower curve with its associated spectra displays the data obtained for the 1223-keV transition from the 2540-keV level. This data gives lower and upper limits for the mean lifetime of the 2540-keV level which imply 17 ± 6 psec.

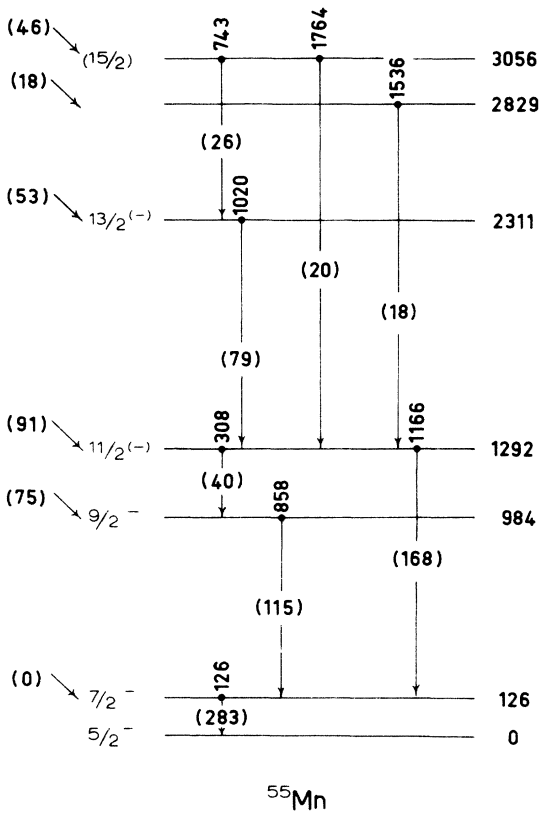

FIG. 6. The level scheme of ^{55}Mn as obtained in the present work. See the caption of Fig. 3 for details.

of the ^{55}Fe 274-keV transition). The peak at channel 403 in the lower spectrum is from a contaminant. The mean lifetime of 382 ± 16 psec which we obtained for this level is in good agreement with a direct electronic timing result of Holland and Lynch[12]: $\tau = 340 \pm 100$ psec. The 1166-keV transition from the 1292-keV level showed no significant evidence for a stop peak, even at the closest target-stopper distance in the RDM measurements. We could, therefore, rigorously limit its mean life to $\tau < 4$ psec. From the DSAM experiment its mean life is $\tau = 1.6 \pm 0.4$ psec. We summarize our results in Table IV. Three of the DSAM lifetimes measured by us in this nucleus are in fair agreement with the lifetimes quoted by Hichwa *et al.*[13]

C. ^{53}Cr

The RDM and DSAM measurements on levels in this nucleus were hampered by the fact that the (^{7}Li, αn) reaction which populated it gave a velocity distribution which was so wide that it was hard to resolve the stopped and shifted peaks in the γ-ray spectrum. This was very different from the (^{7}Li, $p2n$) and (^{7}Li, $3n$) reaction which gave clearly resolved peaks. The substantial difference between the observed recoil velocity and the calculated c.m. velocity has already been remarked upon.

The γ-γ coincidence experiment revealed that in addition to levels seen by Gullholmer and Sawa[14] using the ^{50}Ti(α, n)^{53}Cr reaction we also excited, albeit rather weakly, two further levels at intermediate energies of 2707 and 3244 keV, respectively. We also corroborated the fact that there is a level at 4696 keV which decays to the $\frac{15}{2}^{(-)}$ level at 3084 keV by a 1612-keV γ ray. Due to its weak excitation, the evidence we were able to obtain from the angular distribution data on the multipolarity of this transition was inconclusive. However, the Doppler shift of the photopeak was very small in the DSAM measurement [$F(\tau) < 0.10$], indicating a mean lifetime of greater than 0.8 psec and a possible quadrupole transition. This would support a tentative assignment of $(\frac{19}{2})$ to the level at 4696 keV. We illustrate in Fig. 8 the energy level and decay scheme of ^{53}Cr as determined in the present work. The energy levels in Fig. 8 are split into two groups as presented by Gullholmer and Sawa.[14] Those on the left are believed to be normal shell-model states while the levels on the right, that are connected by cascade γ rays, have been interpreted[14] as possible rotational levels built on a deformed neutron-hole state at 1537 keV.

In Table V we list the γ-ray transitions which are ascribed to ^{53}Cr together with their angular distribution coefficients and intensities. As ex-

TABLE III. γ-ray transitions in ^{55}Mn seen in the ^{51}V(^{7}Li, $2np$)^{55}Mn reactions.

E_γ	E_i	E_f	a_2	a_4	I_γ
126.0 ± 0.1	0.13	0	−0.06 ± 0.01	−0.04 ± 0.01	3253 ± 24
307.9 ± 0.1	1.29	0.98	−0.12 ± 0.02	−0.00 ± 0.02	401 ± 5
743.0 ± 2.0	3.06	2.31	...	...	~260
858.3 ± 0.1	0.98	0.13	+0.06 ± 0.02	−0.07 ± 0.02	1148 ± 14
1019.6 ± 0.2	2.31	1.29	+0.05 ± 0.03	−0.08 ± 0.03	792 ± 13
1166.2 ± 0.1	1.29	0.13	+0.21 ± 0.02	−0.07 ± 0.02	1679 ± 18
1536.3 ± 2.0	2.83	1.29	...	...	~180
1764 ± 2.0	3.06	1.29	+0.33 ± 0.07	−0.07 ± 0.07	~200

TABLE IV. Energies and lifetimes of excited states in ^{55}Mn populated by the ^{51}V(^{7}Li, $2np$)-^{55}Mn reaction.

E_γ (keV)	$F(\tau)$ [a]	τ (psec) This work	τ (psec) Other	τ (psec) Adopted
126.0 ± 0.1	...	382 ± 16 [b]	340 ± 100 [c]	381 ± 16
984.3 ± 0.2	0.20 ± 0.03	1.1 ± 0.3	$0.45^{+0.14}_{-0.09}$ [d]	0.57 ± 0.13
1292.2 ± 0.2	0.14 ± 0.03	1.6 ± 0.4 <4 [b]	$3.3^{+4.1}_{-1.5}$ [d]	1.7 ± 0.4
2311.8 ± 0.3	0.59 ± 0.06	0.20 ± 0.05	0.1 ± 0.04 [d]	0.14 ± 0.03
2828.5 ± 2.0	...	...		
3055.5 ± 2.0	0.50 ± 0.05	0.27 ± 0.06		0.27 ± 0.06

[a] Corrected for feeding from any higher lying levels.
[b] From RDM.
[c] Reference 12.
[d] Reference 13.

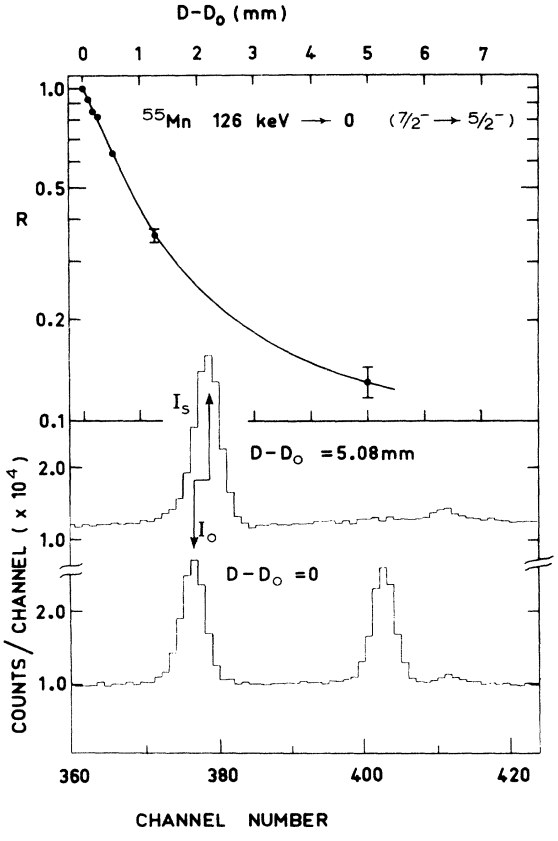

FIG. 7. RDM data obtained for the ground state transition from the 126-keV level in ^{55}Mn. The quantity R which is the ratio of the intensity of the stop peak to the sum of the intensitites of the stopped and shifted peaks was obtained with the use of a program which fitted a sum of two Gaussian peaks to the data. The relative centroid positions and the widths of the two peaks were fixed. The mean lifetime of this level was found to be 382 ± 16 psec.

pected the angular distributions are much less anisotropic than those determined using the ^{50}Ti(α, n) reaction. They are, however, consistent with the spin assignments of Gullholmer and Sawa.[14] We were able to determine the lifetimes of two levels in the RDM experiment. The data we obtained is illustrated in Fig. 9. The 912-keV transition deex-

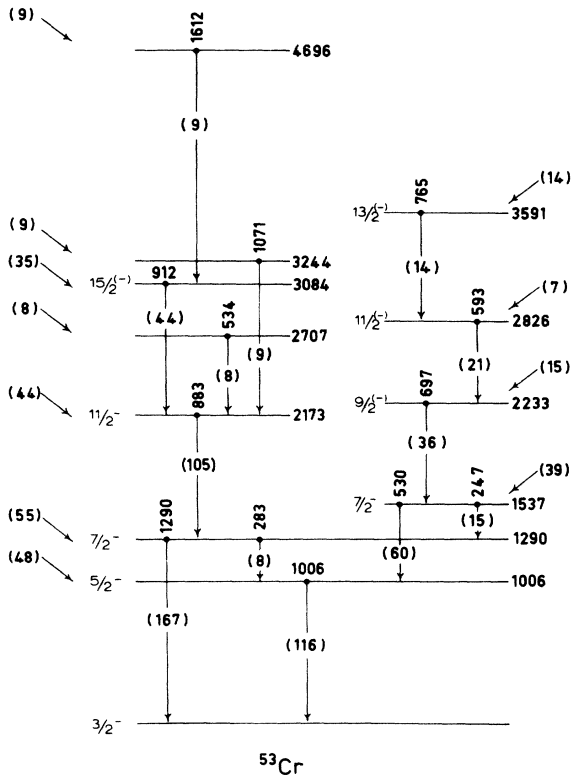

FIG. 8. The energy level scheme of ^{53}Cr as obtained in the present work. See the caption of Fig. 3 for details.

TABLE V. γ-ray transitions in ^{53}Cr seen in the ^{51}V(^{7}Li, αn)^{53}Cr reaction.

E_γ (keV)	E_i	E_f	a_2	a_4	I_γ
247.2 ± 0.2	1.54	1.29	0.10 ± 0.04	0.00 ± 0.04	141 ± 3
283.2 ± 0.2	1.29	1.01	−0.01 ± 0.07	0.03 ± 0.08	73 ± 3
530.2 ± 0.2	1.54	1.01	...	...	...
534 ± 1.0	2.71	2.17	...	...	...
593 ± 1.0	2.83	2.23	...	...	...
696.5 ± 0.3	2.23	1.54	−0.26 ± 0.04	0.02 ± 0.05	357 ± 8
765.2 ± 0.4	3.59	2.83	...	...	...
882.8 ± 0.2	2.17	1.29	+0.14 ± 0.02	−0.06 ± 0.02	1053 ± 12
911.9 ± 0.2	3.08	2.17	+0.10 ± 0.04	+0.01 ± 0.04	443 ± 9
1006.4 ± 0.2	1.01	0	+0.05 ± 0.02	−0.02 ± 0.02	1161 ± 13
1071.4 ± 0.4	3.24	2.17	...	...	...
1289.7 ± 0.2	1.29	0	+0.09 ± 0.02	−0.07 ± 0.02	1674 ± 17
1611.6 ± 2.0	4.70	3.08	−0.11 ± 0.10	+0.16 ± 0.11	~90

citing the 3084-keV level, though weak, showed definite evidence for a mean lifetime of the parent level of 43 ± 15 psec. The data obtained from analysis of the stopped and shifted peaks corresponding to this transition are illustrated in the lower part of Fig. 9. The 883-keV transition deexciting the 2173-keV level also showed an effect due to the lifetime of the 2173-keV level. Analysis of the data in the upper part of Fig. 9 gave a mean lifetime of (47 ± 15) psec for this level. Account has been taken of the feeding via the 3084-keV level. Our result for this lifetime is in disagreement with the result of Engelstein *et al.*[15] who quote $\tau = 6.7 \pm 3.1$ psec. We can give no reason for this discrepancy. If, however, $\tau = 6.7 \pm 3.1$ psec, the most obvious suggestion is that the decay scheme of Fig. 8 is in

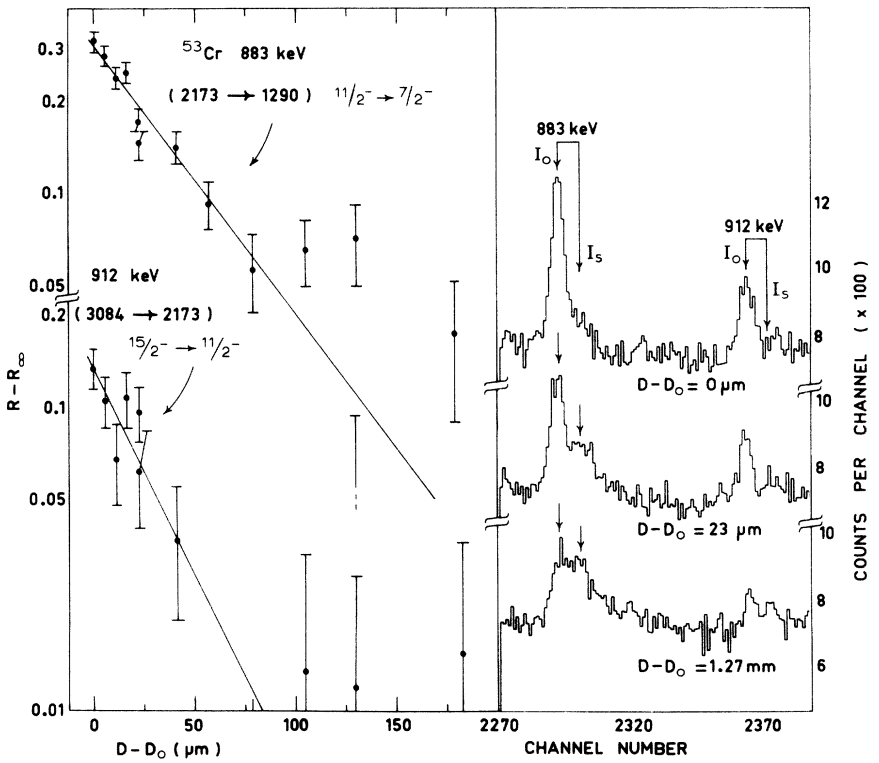

FIG. 9. RDM data obtained for two transitions in ^{53}Cr. Representative partial spectra showing the peaks of interest are displayed on the right of the figure. In the bottom left the data points obtained in an analysis of the 912-keV transition are shown. Analysis of them gives the mean life of the 3084-keV level as $\tau = 43 \pm 15$ psec. Analysis of the data shown in the upper portion of the diagram gives a mean life of 47 ± 15 psec for the 2173-keV level.

TABLE VI. Energies and lifetimes of excited states in ^{53}Cr populated by the ^{51}V(^{7}Li, αn)^{53}Cr reaction.

	τ (psec)			
E_x (keV)	Present work	Other		Adopted
1006.4 ± 0.2	···	>1 [a]	<4 [b]	~2.5
1289.7 ± 0.2	···	1.6 ± 0.2 [c]	<3 [b] <3.5 [d]	1.6 ± 0.2
1536.7 ± 0.3	···	21.5 ± 3.5 [b]	>1.2 [d]	21.5 ± 3.5
2172.5 ± 0.3	47 ± 15	6.7 ± 3.1 [b]	>0.8 [d]	?
2233.2 ± 0.4	$0.4^{+0.4}_{-0.15}$ [e]			$0.4^{+0.4}_{-0.15}$
2706.5 ± 1.1	···			
2826.2 ± 1.1	<1 [f]			<1
3084.4 ± 0.4	43 ± 15			43 ± 15
3243.9 ± 0.5	···			···
3591.4 ± 1.2	···			···
4696.0 ± 2.1	>0.8 [g]			>0.8

[a] T. P. G. Carola *et al.*, Nucl. Phys. A144, 53 (1970).
[b] Reference 15.
[c] Reference 17.
[d] Reference 16.
[e] $F(\tau) = 0.17 \pm 0.08$.
[f] Large Doppler shift observed in angular distribution measurements, but unable to be analyzed quantitatively.
[g] $F(\tau) < 0.10$.

TABLE VII. Radiative transitions in ^{55}Fe. Theoretical comparisons are given for transitions between states belonging to the $(\pi f_{7/2})^{-2}(\nu f_{5/2}, p)$ configurations.

Transition [a] (keV)	Branching ratio [b] (%)	$J_i \rightarrow J_f$	x [c]	$B(E2)_{exp}$ [d] (e^2 fm^4)	$B(M1)_{exp}$ [e] (μ_N^2)	$B(E2)_{th}$ [f] (e^2 fm^4)	$B(M1)_{th}$ [g] (μ_N^2)
1317 → 0(1317)	95 ± 1	$\frac{7}{2} \rightarrow \frac{3}{2}$	$E2$	210 ± 90		132	
→ 931(385)	5 ± 1	$\rightarrow \frac{5}{2}$	0.07 ± 0.03	26^{+26}_{-18}	$0.054^{+0.018}_{-0.026}$	6	1.01
1409 → 0(1409)	44	$\frac{7}{2} \rightarrow \frac{3}{2}$	$E2$	1.1 ± 0.1			
→ 931(477)	56	$\rightarrow \frac{5}{2}$	0.07 ± 0.04	$1.6^{+2.5}_{-1.3}$	0.0051 ± 0.0004		
2212 → 1409(804)	100	$\frac{9}{2} \rightarrow \frac{7}{2}$	0.21 ± 0.02	140 ± 70	0.14 ± 0.07		
2301 → 931(1370)	92 ± 2	$\frac{9}{2} \rightarrow \frac{5}{2}$	$E2$	170 ± 65		38	
→ 1317(984)	8 ± 2	$\frac{9}{2} \rightarrow \frac{7}{2}$	($M1$)		0.0053 ± 0.0021	13	0.07
2540 → 2301(238)	4	$\frac{11}{2} \rightarrow \frac{9}{2}$	$M1$		0.010 ± 0.004	0.4	1.47
→ 1317(1223)	96	$\frac{11}{2} \rightarrow \frac{7}{2}$	$E2$	17 ± 6		108	
2813 → 2540(274)	100	$\frac{13}{2} \rightarrow \frac{11}{2}$	$M1$		0.19 ± 0.4	6	0.25
3419 → 2813(606)	100	$\frac{15}{2} \rightarrow \frac{13}{2}$	−0.07 ± 0.01	490 ± 200	2.5 ± 0.8	43	1.30
5099 → 3419(1681)	100	$(\frac{19}{2}) \rightarrow \frac{15}{2}$	($E2$)	1.9 ± 0.1	$3.7 \times 10^{-4}\gamma$		

[a] The transition is specified by the initial and final energy and the γ-ray energy (all in keV).
[b] From the present work and the results quoted in Refs. 10 and 11.
[c] The mixing ratio for the transition in question, from Ref. 10.
[d] $B(E2) = [813.9/(\tau E_\gamma^5)]$(branching ratio)$\delta$ where $\delta = x^2(1+x^2)^{-1}$. The units are e^2 fm^4 when E_γ is in MeV and τ in psec.
[e] $B(M1) = [0.056\,86/(\tau E_\gamma^3)]$(branching ratio)$\gamma$ where $\gamma = 1 - \delta$. The units are μ_N^2 when E_γ is in MeV and τ in psec.
[f] Horie and Ogawa, Ref. 18. $e_p = 1 + \delta_e$ and $e_n = \delta_e$ where δ_e is taken as 1, and e_p and e_n are the effective proton and neutron charges in units of e.
[g] Horie and Ogawa, Ref. 18. Calculated with the free nucleon g factors.

error. Table VI contains a lifetime summary.

The DSAM measurements gave evidence on the lifetimes of three other levels: the 4696-keV state as previously stated, the 2233-keV level, with a mean lifetime of $0.4^{+0.4}_{-0.15}$ psec, and the 2826-keV level for which we can give a limit of $\tau < 1$ psec. We were unable to extract lifetimes of the 1290- and 1537-keV levels from the data. Engelstein *et al.*[15] quote $\tau = 21.5 \pm 3.5$ psec for the 1537-keV level while Carola and Tamboer[16] give a lower limit of $\tau > 1.2$ psec for this lifetime. Coulomb excitation measurements indicate[17] a mean lifetime of 1.6 ± 0.2 for the 1290-keV level. (See Table VI.)

DISCUSSION

The outstanding characteristic of the fusion-evaporation reactions initiated for instance by ^{7}Li is the selective nature of the excitation; only states lying on or near the yrast line are populated. In the present experiment this has enabled us to populate a level in ^{55}Fe at 6528-keV excitation energy. We suggest that its spin is possibly $\frac{21}{2}$. In ^{55}Mn we suggest a $\frac{15}{2}$ spin for the highest energy state observed at 3056 keV, while in ^{53}Cr a state at 4696 keV is possibly $\frac{19}{2}$. Furthermore, we have been able to determine the lifetimes of a number of the levels. For each of these three nuclei the valence protons are filling the $1f_{7/2}$ shell while the neutrons are in the $(1f_{5/2}, 2p)$ shell. A shell-model study of their spectra, therefore, gives information on the effective neutron-proton force when the neutrons and protons are filling different shells. This problem has been addressed by Horie and Ogawa in two recent papers. In the first[18] they calculated the properties of states belonging to the $(\pi f_{7/2})^{-4} \otimes (\nu f_{5/2}, 2p)$ configuration in ^{53}Cr and the $(\pi f_{7/2})^{-2} \otimes (\nu f_{5/2}, 2p)$ configuration in ^{55}Fe. In a later paper[19] the properties of the states belonging to the $(\pi f_{7/2})^{-3} \otimes (\nu f_{5/2}, 2p)^2$ configuration in ^{55}Mn are treated. Of particular interest from the point of view of the

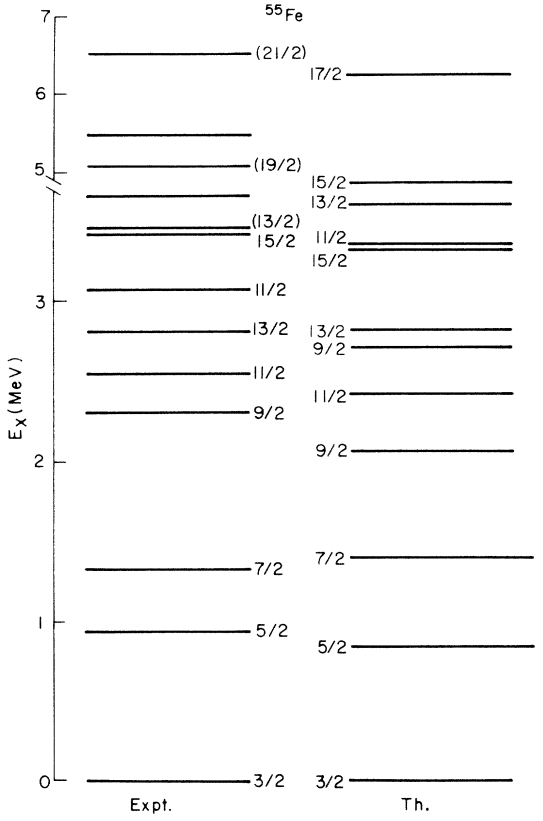

FIG. 10. A comparison between the energy spectra of the high-spin states populated in the present work (labeled expt.) and the predictions of Horie and Ogawa for the $(\pi f_{7/2})^{-2} \otimes (\nu f_{5/2}, 2p)$ configuration (labeled Th.) for the nucleus ^{55}Fe. Suggested spin assignments are bracketed. All levels are, or are assumed to be, of odd parity. Of the levels predicted by Horie and Ogawa, only yrast levels are shown for $J \leq \frac{7}{2}$; while all the levels have been shown for $J \geq \frac{9}{2}$. In the experimental spectrum only those levels which are suspected of belonging to the $(\pi f_{7/2})^{-2} \otimes (\nu f_{5/2}, 2p)$ configuration have been included (i.e., the left-hand scheme of Fig. 3).

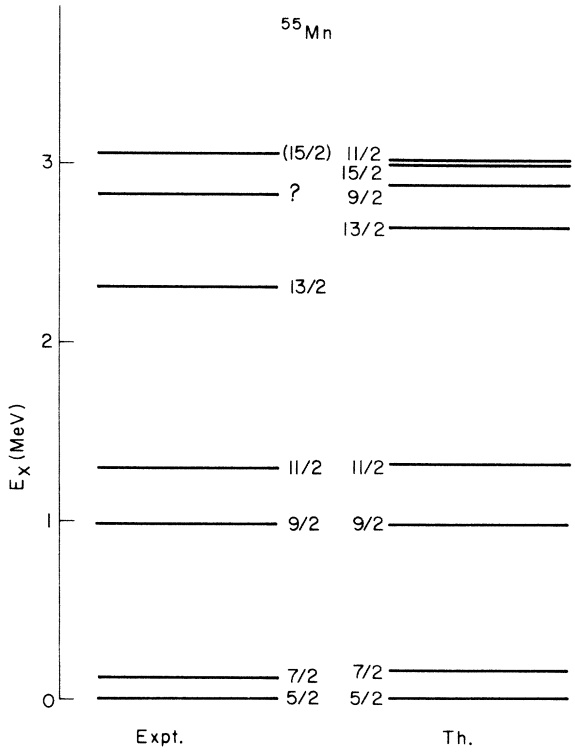

FIG. 11. A comparison between the predictions of Horie and Ogawa for the $(\pi f_{t/2})^{-3} \otimes (\nu f_{5/2}, 2p)^2$ configuration and the experimentally determined level energies for the yrast states in ^{55}Mn. See the caption of Fig. 10 for further details. The unlabeled experimental level at 2.83 MeV could be identified with the theoretically predicted state at 3.00 MeV.

TABLE VIII. Radiative transitions in ^{55}Mn. Theoretical comparisons are given for transitions between states belonging to the $(\pi f_{7/2})^{-3}(\nu f_{5/2},p)^2$ configurations.

Transition[a] (keV)	Branching ratio[b] (%)	$J_i \to J_f$	x[c]	$B(E2)_{exp}$[d] (e^2 fm^4)	$B(M1)_{exp}$[e] (μ_N^2)	$B(E2)_{th}$[f] (e^2 fm^4)	$B(M1)_{th}$[g] (μ_N^2)
126 → 0(126)	100	$\frac{7}{2} \to \frac{5}{2}$	-0.07 ± 0.01	330 ± 100	0.074 ± 0.003	333	0.070
984 → 126(858)	91	$\frac{9}{2} \to \frac{7}{2}$	-0.21 ± 0.03	118 ± 45	$0.14^{+0.04}_{-0.03}$	192	0.106
→ 0(984)	9	$\frac{9}{2} \to \frac{5}{2}$	$E2$	140 ± 35		87	
1292 → 126(1166)	76	$\frac{11}{2} \to \frac{7}{2}$	$E2$	169^{+50}_{-32}		171	
→ 984(308)	24	$\frac{11}{2} \to \frac{9}{2}$	-0.03 ± 0.02	37^{+100}_{-37}	$0.27^{+0.08}_{-0.05}$	177	0.392
2311 → 1292(1020)	100	$\frac{13}{2} \to \frac{11}{2}$	-0.22 ± 0.04	243 ± 90	$0.36^{+0.10}_{-0.07}$	53	0.038
3055 → 1292(1764)	43	$\frac{15}{2} \to \frac{11}{2}$	$E2$	76^{+22}_{-14}		212	
→ 2311(743)	57	$\frac{15}{2} \to \frac{13}{2}$	$(M1)$		$0.29^{+0.09}_{-0.05}$	83	0.524

[a] The transition is specified by the initial and final energy and the γ-ray energy (all in keV).

[b] From the present work and the results quoted in Refs. 10 and 11.

[c] The mixing ratio for the transition in question, from Ref. 10.

[d] $B(E2) = [813.9/(\tau E_\gamma^5)]$(branching ratio)$\delta$ where $\delta = x^2(1+x^2)^{-1}$. The units are e^2 fm^4 when E_γ is in MeV and τ in psec.

[e] $B(M1) = [0.056\,86/(\tau E_\gamma^3)]$(branching ratio)$\gamma$ where $\gamma = 1 - \delta$. The units are μ_N^2 when E_γ is in MeV and τ in psec.

[f] Horie and Ogawa, Ref. 18. $e_p = 1 + \delta_e$ and $e_n = \delta_e$ where δ_e is taken as 1, and e_p and e_n are the effective proton and neutron charges in units of e.

[g] Horie and Ogawa, Ref. 18. Calculated with the free nucleon g factors.

present work is their calculation of the properties of levels of high spin in all three nuclei. We will now discuss the results we have obtained and where possible compare them to the calculations of Horie and Ogawa.[18, 19]

A. ^{55}Fe

Figure 10 compares the energies of the yrast levels observed in the present work with positions of the higher spin states as calculated by Horie and Ogawa.[18] Up to about 3.5-MeV excitation there is an excellent agreement between theory and experiment. The highest spin state which can be formed from the configuration considered by Horie and Ogawa[18] is $\frac{17}{2}$ which they predict at an excitation energy of 5597 keV. Experimentally, either the 3660- or 5476-keV level could have $J = \frac{17}{2}$. There are two states at 5099 and 6528 keV which the experimental evidence indicates have spins greater than $\frac{17}{2}$. It seems possible that these higher spin states arise from promotion of a nucleon from the $1f_{7/2}$ shell to the $(1f_{5/2}, 2p)$ shell. The 1681-keV transition would then correspond to a weak $E2$ transition of 0.15 s.p.u. (single particle unit), which would be consistent with the configurational change. The $(\pi f_{7/2}^{-2}) \otimes (\nu g_{9/2})$ configuration is another possibility for these states.

We summarize the transition matrix elements which can be obtained from a synthesis of our lifetime measurements with previous results in Table VII. We first consider the lower spin levels. The main components of the wave functions of Horie and Ogawa[18, 19] for the four lowest yrast levels are as follows:

$$|\text{g.s.}, \tfrac{3}{2}^-\rangle = |J_p = 0^+ \otimes p_{3/2}; \tfrac{3}{2}^-\rangle ,$$

$$|931\text{ keV}, \tfrac{5}{2}^-\rangle = a\,|J_p = 0^+ \otimes f_{5/2}; \tfrac{5}{2}^-\rangle + b\,|J_p = 2^+ \otimes p_{3/2}, \tfrac{5}{2}^-\rangle ,$$

$$|1317\text{ keV}, \tfrac{7}{2}^-\rangle = |J_p = 2^+ \otimes p_{3/2}; \tfrac{7}{2}^-\rangle ,$$

$$|2301\text{ keV}, \tfrac{9}{2}^-\rangle = c\,|J_p = 2^+ \otimes f_{5/2}; \tfrac{9}{2}^-\rangle + d\,|J_p = 4^+ \otimes p_{3/2}, \tfrac{9}{2}^-\rangle ,$$

plus other small pieces. With these schematic wave functions it is possible to make some qualitative predictions: (1) The $M1$ decay $\frac{5}{2}^- \to \frac{3}{2}^-$ will be inhibited since the transitions between the major components are forbidden. (2) The $M1$ decay $\frac{7}{2}^- \to \frac{5}{2}^-$ should be near normal strength, depending on the amplitude b, while the $E2$ strength for the $\frac{7}{2}^- \to \frac{3}{2}^-$ transition will be comparable to the ^{54}Fe $E2$ strength for the $2^+ \to 0^+$ transition. (3) The $M1$ decay $\frac{9}{2}^- \to \frac{7}{2}^-$ will be inhibited since the transitions between the major components are forbidden while the $E2$ strength for the $\frac{9}{2}^- \to \frac{5}{2}^-$ transition is related by the amplitudes to the ^{54}Fe $E2$ strength for the $4^+ \to 2^+$ and $2^+ \to 0^+$ transitions. For both $E2$ transitions, the $B(E2)$ values would be the same as the

^{54}Fe $2^+ \rightarrow 0^+$ $B(E2)$ values if the wave functions were as given by the first term only. From Table VII and Brown *et al.*[20] we collect the following $B(E2)$ strengths (in $e^2\,\mathrm{fm}^4$):

$$B(E2)_{7/2\rightarrow 3/2} = 210 \pm 90\,,$$

$$B(E2)_{9/2\rightarrow 5/2} = 172 \pm 65\,,$$

$$B(E2)_{2\rightarrow 0} = 102 \pm 4\,,$$

$$B(E2)_{4\rightarrow 2} = 78 \pm 16\,.$$

Considering our neglect of all but the major terms in each wave function, the agreement is not unreasonable. For the $M1$ decays we have: $B(M1)_{7/2\rightarrow 5/2} = 0.054^{+0.018}_{-0.026}\mu_N^2$ and $B(M1)_{9/2\rightarrow 7/2} = 0.0053 \pm 0.0021\,\mu_N^2$. The lifetime of the 931-keV level has not so far been measured. However, the mixing ratio for this transition has been determined[21] as 0.36 ± 0.11 indicating that the $\frac{5}{2}^- \rightarrow \frac{3}{2}^-$ $M1$ transition is probably inhibited. The qualitative predictions of the model are therefore quite reasonable.

We now consider the higher-spin levels as well. Table VII includes theoretical predictions of Horie and Ogawa[18] for transitions connecting states identified as predominantly $(\pi f_{7/2}^{-2})(\nu f_{5/2}, 2p)$. A comparison of the measured $B(E2)$ and $B(M1)$ values to their predictions indicates that quantitative agreement is not good. Obviously more experimental transition strengths are needed and it also appears that the shell-model space is not big enough.

As given in Table VII, a small $E2$ strength was observed for the decay of the $\frac{7}{2}^-$ 1409-keV level to the ground state. This can be explained[10,11] by the fact that a deformed state (Nilsson orbital [303]) based on a two particle-one hole neutron configuration has little overlap with the spherical ground state. No predictions are given for transitions from the deformed states.

B. ^{55}Mn

Horie and Ogawa[19] have presented a calculated level scheme for this nucleus, and also have computed a number of transition strengths. We compare their calculated energies for the higher spin states with the experimental spectrum in Fig. 11. The proton-neutron two-body matrix elements had been determined in a previous calculation[18] by a least squares fit to the observed spectra of the $N = 29$ nuclei assuming ^{48}Ca as an inert core. The agreement between theory and experiment is therefore particularly pleasing. Although the $\frac{13}{2}^-$ level is predicted at an energy of 440 keV above the experimental level at 2.31 MeV, the level which we suppose to be $\frac{15}{2}^-$ at an excitation of 3.06 MeV is within 50 keV of a predicted $\frac{15}{2}$ level at 3.01 MeV. We would not expect to excite the two higher lying $\frac{9}{2}^-$ states predicted by Horie and Ogawa[19] or the $\frac{11}{2}^-$ state at 3.00 MeV. In Table VIII we compare the predictions of Ref. 19 with the experimental transition strengths. For transitions from the $\frac{7}{2}^-$, $\frac{9}{2}^-$, and $\frac{11}{2}^-$ levels the agreement is excellent. The $\frac{7}{2}^- \rightarrow \frac{5}{2}^-$ transition seems to be quite hindered (the $M1$ transition strength is only 0.041 s.p.u.[4]). As Horie and Ogawa[19] point out, this is explained by the fact that the $\frac{7}{2}^-$ state is mainly $|J_p = \frac{7}{2}^- \otimes J_n = 0^+, J = \frac{7}{2}\rangle$ while the $\frac{5}{2}^-$ state is mostly $|J_p = \frac{5}{2}^- \otimes J_n = 0^+, J = \frac{5}{2}\rangle$ and of course an $M1$ transition between these two components is forbidden.[22] The predicted strengths for transitions from the $\frac{13}{2}^-$ and $(\frac{15}{2}^-)$ levels are not in such good accord with the experimental values, nevertheless the agreement is not unreasonable for the $(\frac{15}{2}^-)$ level. The over-all agreement confirms the identification of the predominant configurations.

C. ^{53}Cr

The spectrum calculated by Horie and Ogawa[18] is compared with the experimental energy levels

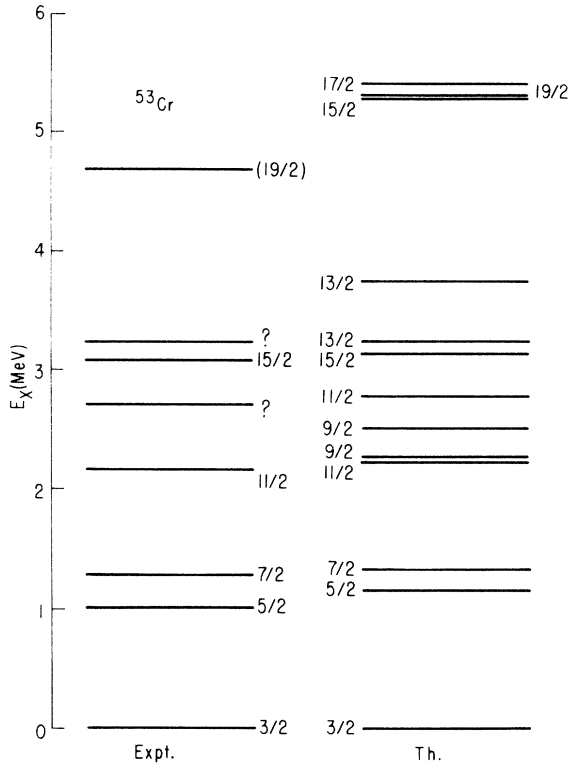

FIG. 12. A comparison between the predictions of Horie and Ogawa for the $(\pi f_{7/2})^{-4} \otimes (\nu f_{5/2}, 2p)$ configuration and the experimentally determined level energies for the high-spin states in ^{53}Cr. See the caption of Fig.10 for further details. In the experimental spectrum only those levels which are suspected of belonging to the $(\pi f_{7/2})^{-4} \otimes (\nu f_{5/2}, 2p)$ configuration have been included (i.e., the left-hand scheme of Fig. 8).

TABLE IX. Radiative transitions in ^{53}Cr. Theoretical comparisons are given for transitions between states belonging to the $(\pi f_{7/2})^{-4}(\nu f_{5/2}, p)^{1}$ configurations.

Transition[a] (keV)	Branching ratio[b] (%)	$J_i \rightarrow J_f$	x[c]	$B(E2)_{exp}$[d] (e^2 fm^4)	$B(M1)_{exp}$[e] (μ_N^2)	$B(E2)_{th}$[f] (e^2 fm^4)	$B(M1)_{th}$[g] (μ_N^2)
1006→ 0(1006)	100	$\frac{5}{2}\rightarrow\frac{3}{2}$	-0.36 ± 0.02	~36	~0.02	69	0.016
1290→1006(283)	5	$\frac{7}{2}\rightarrow\frac{5}{2}$	0.0 ± 0.02	<6	0.078 ± 0.012	0.010	1.43
→ 0(1290)	95	$\frac{7}{2}\rightarrow\frac{3}{2}$	$E2$	136 ± 17		147	
1537→1290(247)	80	$\frac{7}{2}\rightarrow\frac{7}{2}$	0.07 ± 0.03	160^{+170}_{-100}	0.14 ± 0.03		
→1006(530)	20	$\frac{7}{2}\rightarrow\frac{5}{2}$	0.0 ± 0.02	<1	$(3.6\pm0.6)\times10^{-3}$		
2173→1290(883)	100	$\frac{11}{2}\rightarrow\frac{7}{2}$	$E2$	(227^{+190}_{-70})[h] (32 ± 10)[i]		165	
2233→1537(697)	100	$\frac{9}{2}\rightarrow\frac{7}{2}$	0.17 ± 0.03	350 ± 200	0.41 ± 0.04		
2826→2233(593)	100	$\frac{11}{2}\rightarrow\frac{9}{2}$	0.11 ± 0.04	>50	>25		
3084→2173(912)	100	$\frac{15}{2}\rightarrow\frac{11}{2}$	$E2$	30^{+16}_{-11}		135	

[a] The transition is specified by the initial and final energy and the γ-ray energy (all in keV).

[b] From the present work and the results quoted in Refs. 10 and 11.

[c] Reference 14.

[d] $B(E2)=[813.9/(\tau E_\gamma{}^5)]$(branching ratio)$\delta$ where $\delta=x^2(1+x^2)^{-1}$. The units are e^2 fm^4 when E_γ is in MeV and τ in psec.

[e] $B(M1)=[0.056\,86/(\tau E_\gamma{}^3)]$(branching ratio)$\gamma$ where $\gamma=1-\delta$. The units are μ_N^2 when E_γ is in MeV and τ in psec.

[f] Horie and Ogawa, Ref. 18. $e_p=1+\delta_e$ and $e_n=\delta_e$ where δ_e is taken as 1, and e_p and e_n are the effective proton and neutron charges in units of e.

[g] Horie and Ogawa, Ref. 18. Calculated with the free nucleon g factors.

[h] $\tau=6.7\pm3.1$ psec.

[i] $\tau=47\pm15$ psec.

in Fig. 12. The spins labeled with asterisks on the experimental spectrum are those identified by Gullholmer and Sawa[14] as belonging to a rotational band built on the two particle-one hole state at 1537 keV. The agreement for the shell-model states is quite good up to $J^\pi=\frac{11}{2}^-$. Above this spin, the situation is rather confused with two experimental levels of unassigned spin decaying to the $\frac{11}{2}^-$ level at 2173 keV and several levels of high spin predicted by Horie and Ogawa[18] near 3.2 MeV. It is possible that one of the levels at 2707 or 3244 is the $\frac{13}{2}^-$ level predicted in this vicinity while the level at 3084 keV can be identified with the predicted $\frac{15}{2}^-$ level. The weakly excited level at 4696 keV is perhaps to be identified with the $\frac{19}{2}^-$ level predicted at 5.3 MeV. The $\frac{17}{2}^-$ level is predicted to lie slightly above the $\frac{19}{2}^-$ level. If this were actually so, then the most likely decay of the $\frac{19}{2}^-$ level would be to the $\frac{15}{2}^-$ state as observed for the 4696-keV level. If the experimentally determined position of the ^{52}Cr 8^+ state is taken[5] as 4.75 MeV and not 5.2 MeV,[18] then the predicted energies of the $\frac{17}{2}^-$ and $\frac{19}{2}^-$ levels are correspondingly lowered. In this case the agreement in excitation energy of the theoretical $\frac{19}{2}^-$ state with the 4696-keV level is particularly good.

In Table IX we compare the various transition strengths experimentally determined with those calculated by Horie and Ogawa.[18] Agreement is not as good as was the case in ^{55}Mn. Particularly disturbing is the disagreement between experiment and prediction as to the $M1$ strength for the $\frac{7}{2}\rightarrow\frac{5}{2}$ transition. Of the two lifetimes measured for the 2173-keV level, theory favors the shorter. Because of these problems, a definitive comparison must await further experimental investigations of the strengths of the transitions between these levels.

The lifetime obtained[15] for the $\frac{7}{2}^-$ 1537-keV level implies considerable hindrance for transitions to the three shell-model states at lower energies. This is consistent with the suggestion[10] that this state is a deformed state (Nilsson orbital [303]) based on a two particle-one hole neutron configuration as discussed for the $\frac{7}{2}^-$ 1409-keV level in ^{55}Fe. No theoretical predictions are given for these transitions.

The hospitality extended to A. R. Poletti by the Physics Department at both Brookhaven and Stony Brook is warmly appreciated. The authors would like to thank R. McKeown for his help with the analysis of the angular distribution data.

†Work supported in part by the National Science Foundation, the U.S. Atomic Energy Commission, and the New Zealand Universities Research Grants Committee.

*Visiting physicist, State University of New York, Stony Brook, and Brookhaven National Laboratory, January–May 1973.

‡Present address: University of Tokyo, Japan.

[1]An excellent review of nuclear spectroscopy using heavy ion beams with emphasis on the heavier mass region ($A \geq 100$) is by J. O. Newton, Prog. Nucl. Phys. 11, 53 (1970). See also *Proceedings of Heavy-Ion Summer Study*, edited by S. T. Thornton (Oak Ridge National Laboratory, 1973), CONF-720669.

[2]Any one of the statistical models predicts an exponential dependence of the density of states on the excitation energy. The dependence of the density of states on the energy E is often taken as $\omega(E) \approx (E+\delta)^{-2} \times \exp\{2[a(E+\delta)]^{1/2}\}$ where $\delta = 0$ for even-even nuclei, $\delta = \delta_e > 0$ for odd mass nuclei, and $\delta = 2\delta_e$ for odd-odd nuclei. The quantity $\delta_e \approx 0.9$ MeV and $a = A/7.24$ MeV^{-1}. See, for instance, J. R. Grover and J. Gilat, Phys. Rev. 157, 802 (1967).

[3]J. R. Grover, Phys. Rev. 157, 832 (1967).

[4]D. H. Wilkinson, in *Nuclear Spectroscopy, Part B*, edited by F. Ajzenberg-Selove (Academic, New York, 1960), p. 862 ff.

[5]A. R. Poletti, B. A. Brown, D. B. Fossan, and E. K. Warburton, following paper, Phys. Rev. C 10, 2329 (1974).

[6]K. W. Jones, A. Z. Schwarzschild, E. K. Warburton, and D. B. Fossan, Phys. Rev. 178, 1773 (1969).

[7]D. B. Fossan and E. K. Warburton, in *Nuclear Spectroscopy and Reactions, Part C*, edited by J. Cerny (Academic, New York, 1974), p. 307.

[8]For a stretched quadrupole transition from a level of spin J and maximum alignment (all population in the lowest magnetic substate, i.e., either $m = 0$ or $\pm\frac{1}{2}$), $A_2/A_0 \approx \frac{5}{14}[1+3/(2J)]$, with $A_4/A_0 \approx -\frac{1}{10}[1+15/(2J)]$. For a stretched dipole transition, $A_2/A_0 \approx -\frac{1}{4}[1+3/(2J)]$. In all cases terms of order $(1/J)^2$ have been neglected. As the alignment decreases from the maximum, for the quadrupole case A_4/A_0 coefficient decreases towards zero much more quickly than the A_2/A_0 coefficient. It is of interest to note that for the 1681-keV transition in ^{55}Fe (see Table I), $A_2/A_0 = 0.42 \pm 0.02$, while A_2/A_0 evaluated from the above expression is 0.414 (assuming $J = \frac{19}{2}$). In this case the alignment is not likely to be close to the maximum, because of the high spins of the target and projectile. Nevertheless, A_2/A_0 is near the maximum possible, which suggests that these estimates are reasonable even for a limited alignment. The A_4/A_0 coefficients similarly obtained are -0.15 ± 0.02 and -0.179.

[9]C. E. Ragan, III, as referenced in E. K. Warburton, J. W. Olness, and G. A. P. Engelbertink, Phys. Rev. C 7, 170 (1973).

[10]Z. P. Sawa, Phys. Scr. 6, 11 (1972).

[11]B. C. Robertson, G. C. Neilson, and W. J. McDonald, Nucl. Phys. A189, 439 (1972).

[12]R. E. Holland and F. J. Lynch, Phys. Rev. 121, 1466 (1961).

[13]B. P. Hichwa, J. C. Lawson, L. A. Alexander, and P. R. Chagnon, Nucl. Phys. A202, 364 (1973).

[14]W. Gullholmer and Z. P. Sawa, Nucl. Phys. A204, 561 (1973).

[15]P. Engelstein, M. Forterre, N. Schultz, and J. P. Vivien, Nucl. Phys. (to be published).

[16]T. P. G. Carola and J. G. Tamboer, Nucl. Phys. A185, 81 (1972).

[17]R. L. Auble and M. N. Rao, Nucl. Data B3 (Nos. 5–6), 127 (1970).

[18]H. Horie and K. Ogawa, Prog. Theor. Phys. 46, 439 (1971); and private communication.

[19]H. Horie and K. Ogawa, Nucl. Phys. A216, 407 (1973); and private communication.

[20]B. A. Brown, D. B. Fossan, J. M. McDonald, and K. A. Snover, Phys. Rev. C 9, 1033 (1974).

[21]R. W. Bauer and M. Deutsch, Nucl. Phys. 16, 264 (1960).

[22]A. de-Shalit and I. Talmi, *Nuclear Shell Theory* (Academic, New York, 1963), p. 409.